

# **Air Bearing Optimization**

Jennifer Egolf  
Sumanth Swaminathan  
Kyle Spence

## Table of Contents

Introduction.....	3
Governing Equations.....	5
Designs and Solutions.....	11
Laboratory Work.....	20
Conclusions.....	25

## Introduction

Air bearings are non-contact bearings that utilize a thin film of pressurized air to provide a frictionless interface between two surfaces. Applications of air bearings include precision machine tools, semiconductor wafer-processing machines, and other clean-room, high-speed, and precision positioning environments. The non-contact principles of an air bearing provide clear advantages over traditional bearings since problems such as wear are eliminated.

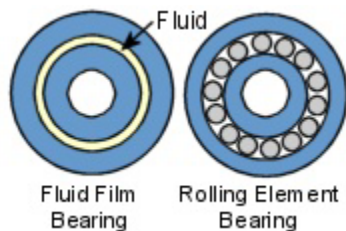


*Figure A.* Air bearing vs. roller bearing. It is noted the type of fluid bearing examined in this document is of planar orientation rather than the rotational bearing shown here.

The goal for this project is to optimize the lift of a planar circular air bearing. Optimizing the bearing will maximize the load that the bearing can accommodate at an applied pressure. The solution to this problem is valuable because it will increase the efficiency of air bearings.

We will begin the optimization by investigating the effect of various patterns etched onto the bottom surface of the bearing. We will start by taking a circular air bearing of fixed dimensions with no etchings and suspending it over a fixed volume of incompressible, constant density air. The bearing hovers over a flat surface due to pressurized airflow introduced to the system. A simplified version of the Reynolds equation will be used to develop a relationship between pressure and the gap height between the bearing and the inlet surface. The height will be a function of the radius. Ultimately, a design that produces optimum lift will be identified. We will also use Newton's Second Law to find a relationship between the pressure and the mass on top of the bearing.

This document will build on theories of lubrication and fluid mechanics to develop optimal designs for an air bearing. Important equations that define our problem were identified through research of previous work in the lubrication field. An annotated bibliography is found in appendix A. Key issues for this problem will be defining all the parameters for optimization, defining the physical bounds of the system's inlet pressure, and developing a method for verification of models. We plan to use numerical methods to observe how pressure is affected by different functions of gap height.

The problem will focus on circular air bearings. Figure B illustrates the basic schematics for a circular air bearing. The bearing floats above the surface due to air pressure through the gap height,  $h$ . The air beneath the bearing acts as a fluid and creates a lubricant film. For this reason, equations of lubrication theory are relevant to this problem. The goal of the project is to maximize the total pressure force under the air bearing by creating channels that “capture” the higher inlet pressure.

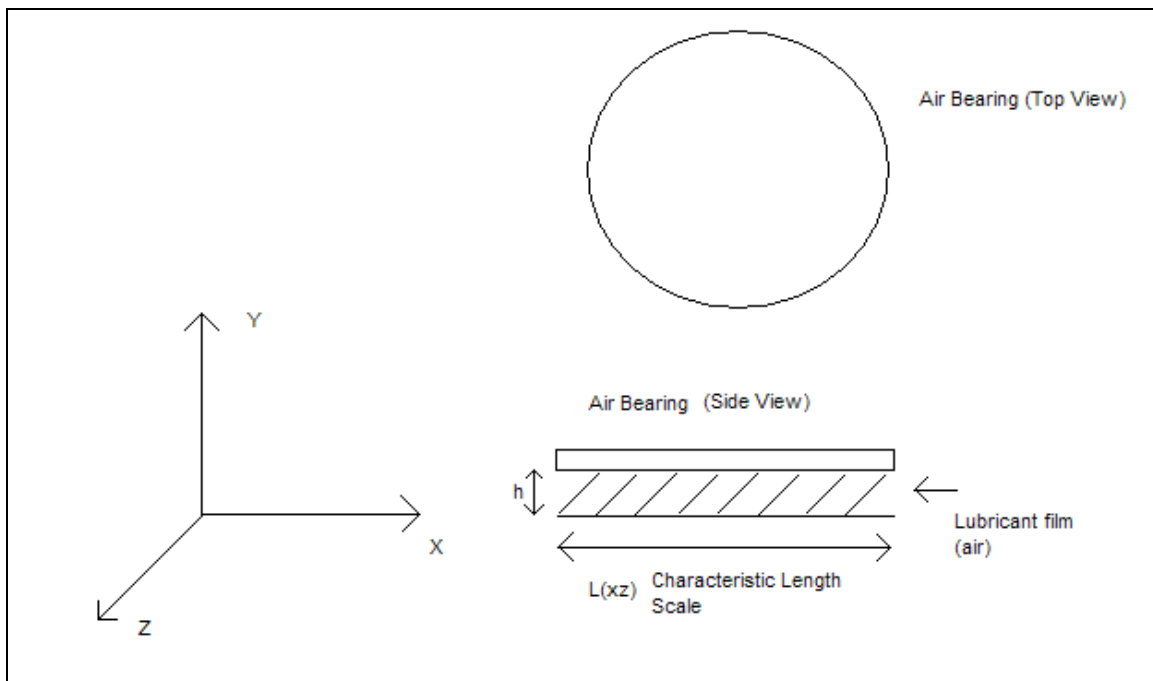


*Figure B:* General schematics for an air bearing. The air bearing we will be discussing is of planar orientation, similar to the idea of an air hockey puck hovering over the surface of the table.

## Governing Equations

We consider a system in which air (treated as a viscous fluid) flows between an air bearing and a flat surface. Optimizing the geometry of the air bearing to achieve the greatest lift from the flowing air is a classical lubrication problem. One model for thin film lubricant flow between two parallel surfaces is the generalized Reynolds equation. We wish to apply this model to our problem, but first we must gain an understanding of its origin. The Reynolds equation is merely a simplified statement of several conservation principles. It is derived by solving the equation of continuity (expresses conservation of mass) simultaneously with the simplified Navier-Stokes Equations (express conservation of linear momentum). The following is meant to show the path from the fundamental conservation principles to Reynolds Equation.

### ***Equation of Continuity***

Let S be a closed surface enclosing a simply connected arbitrary Volume V. We account for the change of mass in the system with two factors. First, we consider the flux. The net mass flow across the closed surface S can be represented by

$$\oint_S (\rho \vec{v}) \cdot \hat{n} dS ,$$

where  $\rho$  = density,

$\vec{v}$  = velocity vector:  $\langle u_x, u_y, u_z \rangle$ ,

$\hat{n}$  = outward unit normal to the surface S and

$dS$  = differential element of surface area.

Second, we consider the possibility of fluid compressibility. That is to say, an increase of mass within a container filled with fluid at all times can occur if and only if the density of the fluid increases. Change in mass due to density variation over time for a given volume takes the following form

$$\int_V \frac{\partial \rho}{\partial t} dV .$$

Mass conservation is then stated as

$$\oint_S (\rho \vec{v}) \cdot \hat{n} dS + \int_V \frac{\partial \rho}{\partial t} dV = 0 .$$

Through use of the divergence theorem, both integrands can be brought to one side, and also because the volume is assumed to be arbitrary, we conclude that the integrand itself must vanish. Thus, we get the *equation of continuity*

$$\frac{\partial \rho}{\partial t} + \text{div}(\rho \mathbf{v}) = 0. \quad (1.1)$$

For the case of an incompressible fluid, the density is assumed to be constant. Thus, it can be pulled out of all derivatives and equation (1.1) simplifies to

$$\frac{\partial v_x}{\partial x} + \frac{\partial v_y}{\partial y} + \frac{\partial v_z}{\partial z} = 0.$$

### ***Navier Stokes Equations***

The Navier-Stokes equations are the general equations of motion for a Newtonian Fluid. Physically, the equations express conservation of linear momentum over some control volume. Although the full mathematical derivation is not shown, we can view each side of the three equations as a portion of the fundamental law of classical mechanics. Recall, Newton's second law alternatively can be stated as

$$\sum \vec{F} = m\vec{a} = \frac{\partial \vec{p}}{\partial t},$$

where  $\sum \vec{F}$  = sum of the forces,

m = mass,

a = acceleration and

$\vec{p}$  = momentum (the tilde is to distinguish from pressure).

Thus, if we sum up all of the parallel and body forces acting on a differential element of fluid (assumed to be the shape of a cube), and we equate those forces to the change in momentum through time, we arrive at *Cauchy's equations of motion*

$$\begin{aligned} \rho \frac{du}{dt} &= \frac{\partial T_{xx}}{\partial x} + \frac{\partial T_{yx}}{\partial y} + \frac{\partial T_{zx}}{\partial z} + \rho f_x, \\ \rho \frac{dv}{dt} &= \frac{\partial T_{xy}}{\partial x} + \frac{\partial T_{yy}}{\partial y} + \frac{\partial T_{zy}}{\partial z} + \rho f_y, \text{ and} \\ \rho \frac{dw}{dt} &= \frac{\partial T_{xz}}{\partial x} + \frac{\partial T_{yz}}{\partial y} + \frac{\partial T_{zz}}{\partial z} + \rho f_z, \end{aligned} \quad (2.1)$$

where:  $T$  = stress,  
 $\rho$  = density,  
 $u$  = velocity in x-direction,  
 $v$  = velocity in y-direction,  
 $w$  = velocity in z-direction and  
 $f$  = body forces.

We then relate stress forces to the velocity by Newton's viscosity relation which states

$$T_{i,j} = \mu \frac{\partial u_i}{\partial x_j}.$$

After some algebraic manipulations and simplifications, we arrive at the Navier-Stokes equations (these are the simplified equations for an incompressible fluid of constant viscosity). They are

$$\begin{aligned} \rho \left( \frac{\partial u}{\partial t} + u \frac{\partial u}{\partial x} + v \frac{\partial u}{\partial y} + w \frac{\partial u}{\partial z} \right) &= -\frac{\partial p}{\partial x} + \mu \left( \frac{\partial^2 u}{\partial x^2} + \frac{\partial^2 u}{\partial y^2} + \frac{\partial^2 u}{\partial z^2} \right) + \rho f_x, \\ \rho \left( \frac{\partial v}{\partial t} + u \frac{\partial v}{\partial x} + v \frac{\partial v}{\partial y} + w \frac{\partial v}{\partial z} \right) &= -\frac{\partial p}{\partial y} + \mu \left( \frac{\partial^2 v}{\partial x^2} + \frac{\partial^2 v}{\partial y^2} + \frac{\partial^2 v}{\partial z^2} \right) + \rho f_y, \text{ and} \\ \rho \left( \frac{\partial w}{\partial t} + u \frac{\partial w}{\partial x} + v \frac{\partial w}{\partial y} + w \frac{\partial w}{\partial z} \right) &= -\frac{\partial p}{\partial z} + \mu \left( \frac{\partial^2 w}{\partial x^2} + \frac{\partial^2 w}{\partial y^2} + \frac{\partial^2 w}{\partial z^2} \right) + \rho f_z. \end{aligned} \quad (3.1)$$

### ***Scaling Navier Stokes***

The geometry of lubricant films is of particular use in making simplifications of the Navier-Stokes equations. That is to say, we wish to scale this equation for the sake of first, generalizing the system without dimensions, and second, eliminating terms that can be assumed small. Because the geometry is assumed to have very small curvature in comparison to its length, with a much larger in-plane dimension than thickness, when we scale the equation, several terms become extremely small. First, the choice of scalings should be indicated as

$$\tilde{x} = \frac{x}{L_{xz}}; \tilde{y} = \frac{y}{L_y}; \tilde{z} = \frac{z}{L_{xz}},$$

where:  $L_{xz}$  = length scale of lubricant film in (x,z) plane and  
 $L_y$  = length scale across thickness (recall, thickness is in y-direction).

We similarly normalize the velocity with the scales

$$\tilde{u} = \frac{u}{U_*}; \tilde{v} = \frac{v}{V_*}; \tilde{w} = \frac{w}{U_*}.$$

Now, we can get an idea of how large  $V_*$  is relative to  $U_*$  by plugging these scalings into the equation of continuity and matching order of coefficients which gives

$$\frac{\partial \tilde{u}}{\partial \tilde{x}} + \left( \frac{V_* L_{xz}}{U_* L_y} \right) \frac{\partial \tilde{v}}{\partial \tilde{y}} + \frac{\partial \tilde{w}}{\partial \tilde{z}} = 0.$$

Now, the ratio of the planar scaling to the thickness scaling can vary based on the system.

A decent approximation for the ratio is

$$\frac{L_y}{L_{xz}} = o(10^{-3}).$$

The length scale in the y-direction is  $10^{-3}$  or less times that of the length scale in the x-z plane. Thus, in order for every term in the continuity equation to be important, the magnitude of the velocity scale in the y-direction must be of equal proportion to the magnitude of the velocity scale in the x or z directions. This will make the coefficient in front of the velocity time derivative in the y-direction  $O(1)$  which gives

$$V_* = \left( \frac{L_y}{L_{xz}} \right) U_* .$$

Finally, we must scale pressure and time. We define the non-dimensional quantities for pressure and time as follows,

$$\tilde{p} = \text{Re} \left( \frac{L_y}{L_{xz}} \right) \left( \frac{p}{\rho U_*^2} \right),$$

$$\tilde{t} = \Omega t, \text{ and}$$

$$\text{Re} = \frac{t_i}{t_v} = \frac{U_* L_y}{\nu},$$

where  $\Omega$  = natural time scale,  
 $\nu$  = kinematic viscosity,  
 $t_i$  = random inertial flow and  
 $t_v$  = viscous flow.

In these scalings, 'Re' is defined as the Reynolds number. Physically, it represents the ratio of forces associated with inertial flow to viscous flow. That is to say, if the fluid is not laminar and there is much random motion, the Reynolds number would be larger.

Often, the Reynolds number is convenient because it is easy to simplify a system in such a way as to make the Reynolds number very small or very large.

If we plug in all the chosen scalings and the reduced Reynolds number and time scalings it gives

$$\hat{\Omega} = \frac{L_y^2 \Omega}{\nu}; \hat{\text{Re}} = \text{Re} \left( \frac{L_y}{L_{xz}} \right).$$

We get the scaled Navier-Stokes equations

$$\hat{\text{Re}} \left( \frac{\partial \tilde{u}}{\partial \tilde{t}} + \tilde{u} \frac{\partial \tilde{u}}{\partial \tilde{x}} + \tilde{v} \frac{\partial \tilde{u}}{\partial \tilde{y}} + \tilde{w} \frac{\partial \tilde{u}}{\partial \tilde{z}} \right) = -\frac{\partial \tilde{p}}{\partial \tilde{x}} + \frac{\partial^2 \tilde{u}}{\partial \tilde{y}^2}, \text{ and}$$

$$\hat{\text{Re}} \left( \frac{\partial \tilde{w}}{\partial \tilde{t}} + \tilde{u} \frac{\partial \tilde{w}}{\partial \tilde{x}} + \tilde{v} \frac{\partial \tilde{w}}{\partial \tilde{y}} + \tilde{w} \frac{\partial \tilde{w}}{\partial \tilde{z}} \right) = -\frac{\partial \tilde{p}}{\partial \tilde{z}} + \frac{\partial^2 \tilde{w}}{\partial \tilde{y}^2}.$$

These scalings, of course, were very important in that they allowed us to eliminate the equation for pressure variation in the y-direction. Now we have a set of 2 equations, which in addition to the equation of continuity, gives 3 equations and 3 unknowns. Now, we have a well posed problem, and can attempt to solve the equations.

### ***Reynolds Equation***

#### Assumptions

- 1) Constant viscosity, Newtonian lubricant
- 2) Thin film geometry
- 3) Negligible inertial ( $\hat{\text{Re}}=0$ )
- 4) Negligible body forces

When the above assumptions are applied to the scaled equations of motion, we get the following set of equations

$$\frac{\partial p}{\partial x} = \mu \frac{\partial^2 u}{\partial y^2},$$

$$\frac{\partial p}{\partial z} = \mu \frac{\partial^2 w}{\partial y^2}, \text{ and}$$

$$\frac{\partial u}{\partial x} + \frac{\partial v}{\partial y} + \frac{\partial w}{\partial z} = 0.$$

Since neither of the pressure gradient terms varies across the thickness, the first two equations can be integrated twice subject to the following boundary conditions which gives

$$u(0) = U_1; u(h) = U_2, \text{ and} \\ w(0) = 0; w(h) = 0.$$

We solve for u and w and get

$$u = \frac{1}{2\mu} \frac{\partial p}{\partial x} (y^2 - yh) + \left(1 - \frac{y}{h}\right) U_1 + \frac{y}{h} U_2, \text{ and} \\ w = \frac{1}{2\mu} \frac{\partial p}{\partial z} (y^2 - yh).$$

Now, from here, we cannot directly plug u and w into the equation of continuity and integrate because we would have both p and v unknown. We solve this problem by averaging v over the thickness and integrating all other terms in the equation with respect to y. This gives

$$[v]_{y=0}^{y=h(x,t)} = - \int_0^{h(x,t)} \frac{\partial u}{\partial x} dy - \int_0^{h(x,t)} \frac{\partial w}{\partial z} dy. \quad (4.1)$$

We represent the averaged velocity across the thickness as

$$[v]_{y=0}^{y=h(x,t)} = -(V_1 - V_2) = \frac{dh}{dt}.$$

Finally, we plug our values for u and w into (5.1) and integrate. After some simplification, we get the generalized Reynolds Equation

$$\frac{\partial}{\partial x} \left( \frac{h^3}{\eta} \frac{\partial p}{\partial x} \right) + \frac{\partial}{\partial y} \left( \frac{h^3}{\eta} \frac{\partial p}{\partial y} \right) = 6h \frac{\partial}{\partial x} (U_1 + U_2)h + 6(U_1 - U_2) \frac{\partial h}{\partial x} + 12 \frac{\partial h}{\partial t}, \quad (4.2)$$

where h = Gap height,  
 $\eta$  = Fluid viscosity,  
 $U_i$  = Velocity at boundary (with respect to x),  
 $V_i$  = Velocity at boundary (with respect to x),  
P = Pressure and  
z = direction of the height (dimension coming out of the page).

Reynolds equation in lubricant pressure is the mathematical statement of the classical theory of lubrication. Physically, it can be thought of as an expression of conservation principles for a system made up of lubricant flow between two parallel surfaces. The terms on the left-hand side of the equation represent flow due to pressure gradients across the domain, while the terms on the right hand side represent flows induced by motions of the bounding surfaces and shear induced flow by the sliding velocities  $U$  and  $V$ . For our purposes, we assume no such motions of the bounding surfaces, and also no time dependence.

### Designs & Solutions

Manipulation of the Reynolds equation is quite difficult without knowledge of the geometry of the system. The geometry of the system cannot be achieved without a known design for the bearing. Thus, we will not be optimizing the design of the bearing subject to the Reynolds equation; rather we will be using the Reynolds equation to find the lift coefficient once a design has been chosen. The hope is that we can study and optimize the lift coefficient once an analytical expression for it is found through the Reynolds equation.

### Fundamental Assumptions (for all cases)

- 1) Steady Flow
- 2) No motion of the bounding surfaces ( $U=V=0$ ).
- 3) No Pressure gradients in the direction of the gap height ( $y$ -direction)

In cylindrical coordinates, the non-dimensional Reynolds Equation takes the form

$$\bar{\nabla} \cdot (h^3 \nabla p) = 0. \quad (5.1)$$

Assumptions 1 and 2 allow for the elimination of all terms on the right hand side of the generalized Reynolds equation. Assumption three eliminates pressure gradients in the  $y$ -direction and after conversion to cylindrical coordinates, we are left with equation (5.1).

### ***Flat Bearing***

In the case of the flat bearing, we assume an axi-symmetric pressure function and a constant height, so that we may simplify and solve (5.1) as

$$\begin{aligned}\frac{d}{dr}\left(r\frac{dp}{dr}\right) &= 0, \\ r\frac{dp}{dr} &= A, \\ \frac{dp}{dr} &= \frac{A}{r}, \text{ and} \\ p(r) &= A\ln(r) + B.\end{aligned}$$

Now, for the sake of continuity, we must define the boundary conditions in such a way as to eliminate singularities on the domain. The natural log function is not defined at the origin, so we define an area  $r < \varepsilon$  where the pressure is set as the inlet pressure. [We also allow for an epsilon because any reasonable reproduction of the physical problem would require an initial flow of air to have some radius.] Otherwise, the feed tube would be infinitely small. Thus, we solve for A and B by first stating

$$p(\varepsilon) = p_{in}; p(R) = p_{atm}.$$

Plugging in these boundary conditions, we find that

$$\begin{aligned}p_{in} &= A\ln(\varepsilon) + B, \text{ and} \\ p_{atm} &= A\ln(R) + B.\end{aligned}$$

$$\therefore A = \frac{\Delta p}{\ln(R/\varepsilon)}; B = P_{atm} - \frac{\Delta p}{\ln(R/\varepsilon)}(\ln(R)).$$

(Where  $\Delta p = p_{in} - p_{atm}$ .)

Now, we write the resulting solution in piecewise form as

$$\begin{aligned}P(r) &= P_{in} && \text{if } r < \varepsilon \text{ and} && (6.1) \\ P(r) &= \frac{\Delta P}{\ln(R/\varepsilon)} \ln\left(\frac{r}{R}\right) + P_{atm} && \text{if } \varepsilon \leq r \leq R.\end{aligned}$$

With an explicit function for the pressure, we can formulate an expression for the lift by evaluating the following integral over all pieces of the radial domain. This gives

$$L = \iint_{\Omega} (p(r) - p_{atm}) dA.$$

For our case we have

$$L = \int_0^{2\pi} \int_0^{\varepsilon} (\Delta p) r dr d\theta + \int_0^{2\pi} \int_{\varepsilon}^R \frac{\Delta p}{\ln(R/\varepsilon)} \ln\left(\frac{r}{R}\right) r dr d\theta, \text{ and} \quad (6.2)$$

$$L = \frac{1}{2} \pi \frac{\Delta p}{\ln(R/\varepsilon)} (R^2 - \varepsilon^2).$$

Finally, we relate pressure to the amount of applied weight by concluding that in order for the bearing to hover at a constant height, the lift force associated with the applied pressure must equal the force of weight pushing down. Newton's second law says:  $F=ma$ . Thus, we conclude that  $L=mg$  (for  $g$  = gravitational force). Substituting this equation into our expression for the lift and solving for  $\Delta P$  we find

$$\Delta p = \frac{2g \ln(R/\varepsilon)}{\pi(R^2 - \varepsilon^2)} M. \quad (6.3)$$

For the initial investigation of an air bearing without any etchings on the bottom surface, the pressure distribution is expected to behave as illustrated below in Figure C. The arrows indicate pressure levels with the taller arrows being of the highest pressure, namely the inlet pressure. Pressure under the air bearing should be the inlet pressure at the center of the bearing where the flow is entering, and decrease logarithmically towards atmospheric pressure as the edge of the bearing is approached. The magnitude of the distribution should vary depending on the weight of the bearing, having higher pressures for increased load.

Since the goal of the project is to maximize the total pressure force under the air bearing by creating channels that "capture" the higher inlet pressure, the optimum solution may have a very different pressure distribution than the simple case shown below.

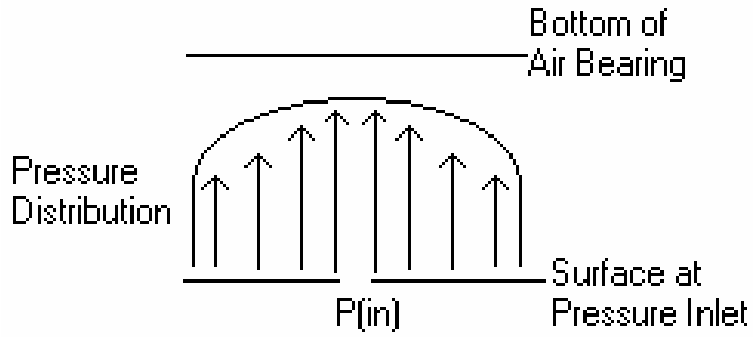
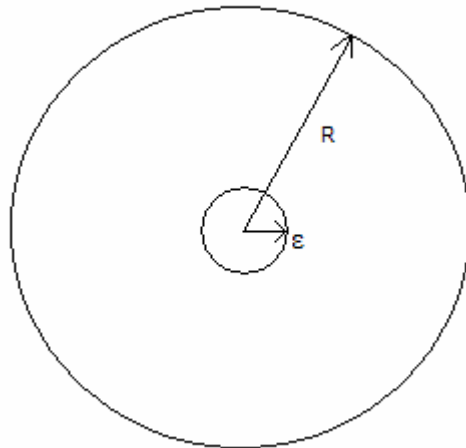


*Figure C:* Theoretical pressure distribution for a flat air bearing.

At the perimeter of the bearing, the pressure is equal to atmospheric pressure and at the center, within the limits of epsilon; the pressure is equal to the inlet pressure. In order to use these boundary conditions, a value for  $\epsilon$  must be determined. Through laboratory experiments we should be able to define  $\epsilon$  using equation 6.3. Using the slope of the line for pressure vs. mass and the known radius of the bearing,  $\epsilon$  should be easily obtained.



*FigureD:* Underside of air bearing with radius ( $R$ ) and radius of inlet pressure ( $\epsilon$ ) noted.

## Annular Bearing

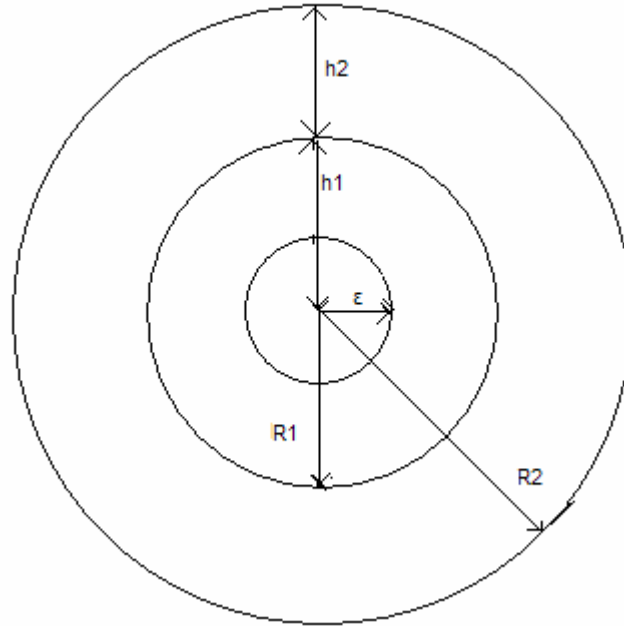


Figure E: Underside of air bearing with radius ( $R_1$  and  $R_2$ ) and radius of inlet pressure ( $\varepsilon$ ) noted. Also noted are corresponding heights: ( $h_1$  and  $h_2$ )

The assumptions and parameters for this model are the same as those of the flat case with one important additional feature. There is of course height dependence in the equation, but as is shown in Figure E, the height dependence is uniformly distributed over two regions. That is to say, the height is constant along the annulus and is constant along the inside disc. This allows us to obtain a piecewise analytical solution of the system. Let  $R_1$  and  $R_2$  denote the inner and outer radii of the bearing with their respective height functions  $h_1$  and  $h_2$ . We know that if we define  $h$  piece-wise in this manner, there is a discontinuous jump at the edge of the annulus ( $R_1$ ). We therefore tie the solutions together by establishing the boundary condition

$$\lim_{r^+ \rightarrow R_1} h_1^3 \frac{\partial p}{\partial r} = \lim_{r^- \rightarrow R_1} h_2^3 \frac{\partial p}{\partial r}. \quad (7.1)$$

Our pressure function then takes the form

$$\begin{aligned} p(\varepsilon \leq r \leq R_1) &= A \ln(r) + B, \text{ and} \\ p(R_1 \leq r \leq R_2) &= C \ln(r) + D. \end{aligned} \quad (7.2)$$

Just as before, we let the inlet pressure be constant over a disc of radius  $\varepsilon$  (this disc representing the area covered by the pipe head), and we let the pressure at the boundary ( $r=R_2$ ) be atmospheric pressure. Plugging these boundary conditions into (7.2) and then plugging that result into (7.1), we find that

$$\begin{aligned} A \ln(\varepsilon) + B &= p_{in}, \\ C \ln(R_2) + D &= p_{atm}, \end{aligned} \quad (7.3)$$

$$\frac{C}{R_1} h_2^3 = \frac{A}{R_1} h_1^3,$$

$$\left( \frac{h_2}{h_1} \right)^3 C = A,$$

$$H = \left( \frac{h_2}{h_1} \right), \text{ and}$$

$$H^3 = \frac{A}{C}.$$

Conditions of continuity across the underside of the bearing ensuring that there are no singularities at  $r = R_1$  imply that

$$A \ln(R_1) + B = C \ln(R_1) + D$$

and

$$A \ln(R_1) + B = C \ln(R_1) + p_{atm} - C \ln(R_2).$$

We can then solve for the four coefficients which are

$$A = \frac{H^3 \Delta P}{\ln \left[ \frac{R_1^{H^{-3-1}} \varepsilon}{R_2^{H^{-3}}} \right]},$$

$$B = p_{in} - A \ln(\varepsilon),$$

$$C = \frac{\Delta P}{\ln \left[ \frac{R_1^{H^{-3-1}} \varepsilon}{R_2^{H^{-3}}} \right]}, \text{ and}$$

$$D = p_{atm} - C \ln(R_2).$$

Using these coefficients, we have a piece-wise analytical solution for  $p(r)$ . That solution is

$$\begin{aligned}
p(r < \varepsilon) &= p_{in}, \\
p(\varepsilon \leq r \leq R_1) &= \frac{H^3 \Delta p}{\ln\left(\frac{\varepsilon R_1^{(H^3-1)}}{R_2^{(H^3)}}\right)} \ln\left(\frac{r}{\varepsilon}\right) + p_{in}, \text{ and} \\
p(R_1 \leq r \leq R_2) &= \frac{\Delta p}{\ln\left(\frac{\varepsilon R_1^{(H^3-1)}}{R_2^{(H^3)}}\right)} \ln\left(\frac{r}{R_2}\right) + p_{atm}.
\end{aligned} \tag{7.4}$$

Integrating piece-wise and summing as with the flat bearing, we find that

$$L = \left(\frac{\pi}{2}\right) \frac{\Delta p}{\ln\left(\frac{R_1 R_2^{(H^3-1)}}{\varepsilon^{H^3}}\right)} \left[ (H^3 - 1)R_2^2 + R_1^2 - \varepsilon^2 \right]. \tag{7.5}$$

Finally, letting  $L = mg$  under the assumption that at equilibrium, the bearing must exactly counteract the applied mass and its own mass, we find our expression for the pressure drop under the bearing as

$$\Delta p = \frac{2g \ln\left(\frac{R_1 R_2^{(H^3-1)}}{\varepsilon^{H^3}}\right)}{\pi \left[ (H^3 - 1)R_2^2 + R_1^2 - \varepsilon^2 \right]} M. \tag{7.6}$$

Integrating piece-wise and summing (see Appendix G) as with the flat bearing, we find that

$$L = \frac{\pi \Delta P}{2} \left[ \frac{R_1^2 (1 - H^3) + H^3 \varepsilon^2 - R_2^2}{\ln\left[\frac{R_1^{H^3-1} \varepsilon}{R_2^{H^3}}\right]} \right]. \tag{7.5}$$

Finally, letting  $L = mg$  under the assumption that at equilibrium, the bearing must exactly counteract the applied mass and its own mass, we find our expression for the pressure drop under the bearing as

$$\Delta p = \frac{2Mg}{\pi} \left[ \frac{\ln \left[ \frac{R_1^{H^3-1} \varepsilon}{R_2^{H^3}} \right]}{R_1^2 (1-H^3) + H^3 \varepsilon^2 - R_2^2} \right]. \quad (7.7)$$

### **Optimization**

In order to optimize the annular case, we first make the terms in Equation 7.7 non-dimensional.  $H$  is already non-dimensional, as it is the ratio of  $h_2$  to  $h_1$ . The inner radius ( $R_1$ ), the outer radius ( $R_2$ ), and the radius of the inlet pressure ( $\varepsilon$ ) will be scaled with respect to the radius of the bearing. Mass ( $M$ ) is scaled with the mass of the bearing.

$$\tilde{p} = \frac{\Delta p}{p_c}; \tilde{M} = \frac{M}{M_c}; \tilde{R}_1 = \frac{R_1}{R}; \tilde{R}_2 = \frac{R_2}{R}; \tilde{\varepsilon} = \frac{\varepsilon}{R},$$

which leads to the non-dimensional solution:

$$\tilde{p} = \frac{2}{\pi} \frac{\ln(\tilde{R}_1^{(H^3-1)} \tilde{\varepsilon})}{[\tilde{R}_1 (1-H^3) + H^3 \tilde{\varepsilon}^2 - 1]} \tilde{M}. \quad (8.1)$$

This solution reduces to

$$\tilde{p} = \frac{2}{\pi} \left[ \frac{\ln \tilde{\varepsilon}}{\tilde{\varepsilon}^2 - 1} \right] \tilde{M}$$

for  $H=1$  (flat bearing case), which is consistent with the non-dimensional version of Equation (6.3) where  $R$  is simply equal to 1.

In order to find an optimum solution for the annular case, it is necessary to declare a condition of constant volume under the bearing. In this way, an adjustment in the placement of the annulus, which is simply the chosen magnitude of  $R_1$ , causes an adjustment in the thickness of the annulus. The volume constraint is written as

$$\frac{1}{h_2}[\pi R^2 \tilde{R}_1^2 h_1 + \pi R^2 \tilde{R}_2^2 h_2 - \pi R^2 \tilde{R}_1^2 h_2] = \frac{V_m}{h_2}. \quad (8.2)$$

(Where  $V_m$  is a constant for the minimum volume)

Recall that  $H = \left(\frac{h_2}{h_1}\right)$  and equation 8.2 reduces to

$$\tilde{R}_1^2 \left(\frac{1}{H} - 1\right) = \frac{V_m}{R^2 \pi h_2} - 1, \text{ and}$$

$$V_m = \pi R^2 h_i.$$

where  $h_i$  is the minimum height for the flat bearing case. This leads us to the simple relationship

$$\tilde{R}_1^2 \left(\frac{1}{H} - 1\right) = \frac{h_i}{h_2} - 1 = C. \quad (8.3)$$

For the initial investigation of equation 8.3, the constant  $V_m$  is assumed as the minimum volume for the flat bearing case where  $h_i$  is equal to 0.002 inches. Then,  $h_2$  is quantified as the minimum height for the annular case, 0.001 inches. The constant,  $C$ , is then equal to one and equation 8.3 is easy to work with.

The group is currently using a MATLAB code that, when given a height input, will solve for pressure using spectral methods. Spectral methods will allow for numerical solutions over an irregularly shaped grid, a circle in this case, and will do so with relatively quick convergence. The program is based on the general and more difficult case of Reynolds equation that allows the pressure and height to have both radial and angular dependence. In order to use the general, non-dimensional form of Reynolds Equation in the computer program it was necessary to solve out the terms in equation 5.1. Using Maple (appendix B), the equation was found as

$$\frac{\partial^2 p}{\partial r^2} (h^3) + \frac{\partial p}{\partial r} \left( \frac{h^3}{r} + 3h^2 \frac{\partial h}{\partial r} \right) + \frac{\partial^2 p}{\partial \theta^2} \left( \frac{h^3}{r^2} \right) + \frac{\partial p}{\partial \theta} \left( 3 \frac{h^2}{r^2} \frac{\partial h}{\partial \theta} \right) = 0. \quad (9.1)$$

Using the constant volume constraint with  $C=2$ , the MATLAB program was used to predict the lift for several different annular schemes. The program was run using non-dimensional inputs coordinating to the inner radii for the annulus being equal to 1.27 cm, 1.91 cm, 2.54 cm, 3.175 cm, and 4.445 cm. The results of these trials are shown below in Figure F. It is interesting to note that the lift, which we are trying to maximize, does not follow a linear trend as the radius of the annulus increases. Rather, the relationship is unclear and the optimal annulus must be found by optimizing equation (8.1) subject to the volume constraint.

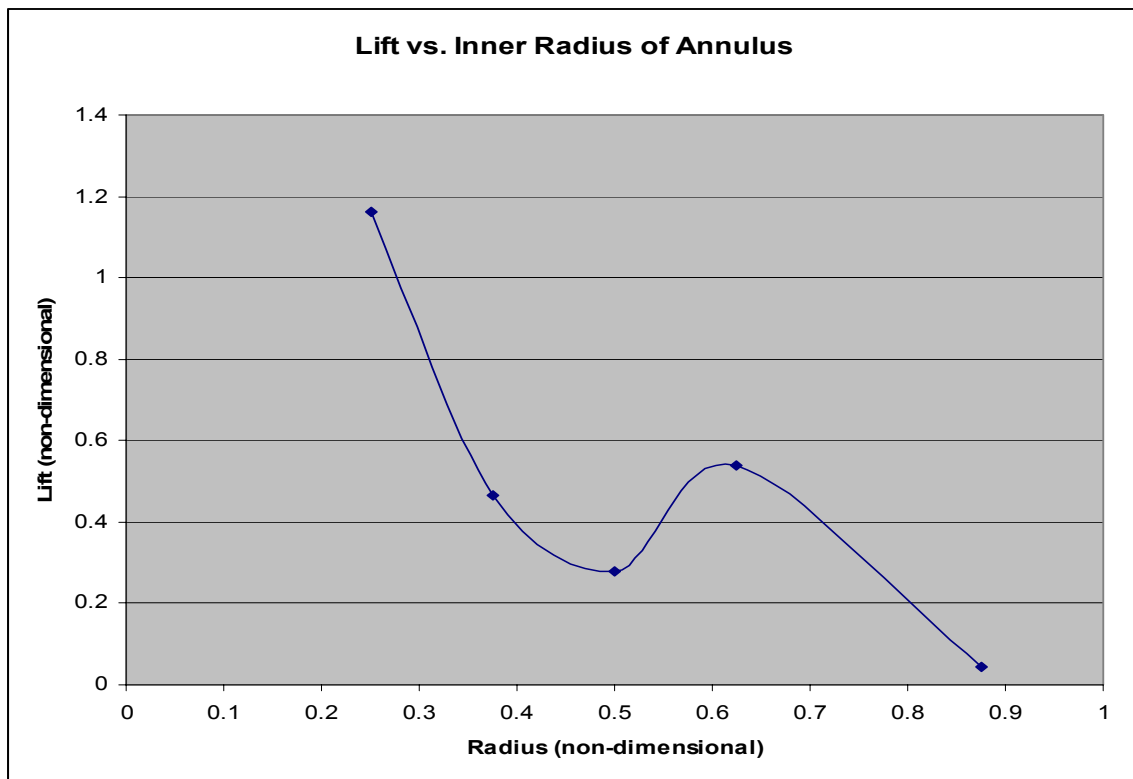


Figure F. MATLAB results for several annular schemes. Non-dimensional values for  $H$ ,  $\epsilon$ , and the inner and outer radii were used in the program.

## Laboratory Work

### *Introduction*

The purpose of our laboratory experiments is to give us a better understanding of our problem and to assist us in solving it. In the experiments we test various bearings with different etching patterns. We show that there is a linear relationship between pressure and applied mass for any etching carved into the bottom of the air bearing. This allows us to find better designs and predict the pressure for certain masses applied to an air bearing. Essentially, the shallower the slope of the pressure vs. applied mass plot, the better the design.

We ran into some difficulties when we first started our lab experiments. The epoxy bond that held the pressure fitting to the flat surface leaked and then broke off. This required that we refit our apparatus before we could proceed with our experiments.

### ***Procedure***

A pressure fitting forces air through a hole in a glass disk upon which the air bearing floats. A pressure sensor is attached to the pressure valve and provides a reading of the pressure under the bearing. Different bearing designs are made using four and six inch glass bearings with shim stock applied to the bottom surfaces to simulate etchings.

The bearings are placed onto the pressure feeding surface and several small masses are applied all at once. Then the pressure valve is opened and the data recording program is run. The small masses are then removed one by one allowing a period of time to pass between each loading case. Once all the masses are removed and data for the case of no applied mass is recorded, a different bearing is then tested with the same masses and same flow rate as was just used. This is repeated for all the bearings to be tested at that time.

### ***Results***

#### **Experiment 1**

Our first time in the lab we ran 3 different experiments; one to record the ambient pressure, one with a flat bearing of diameter 10.16 cm with different mass loadings of 0, 0.5, 0.7, 0.9 and 1.0 kg, and one with a bearing with an annulus of inner radius of 2.54 cm with the same mass loadings as the flat bearing. When we ran the experiments, we

tried to maintain the same gap height underneath the bearing during each experiment. This was done by adjusting the pressure coming into the system. We recorded data for each bearing in the form of pressure versus time. We then averaged the pressure for a certain time with an applied mass and used that to construct a plot of pressure versus mass. We hoped that this would show a linear relationship between pressure and mass. However, the plots do not show a linear relationship very well, as can be seen in Appendix C, Figures 2 and 3. This could be due to the fact that there were many sources of error. For example, our instrument for measuring height allowed for very little precision in our measurements. Furthermore, there could have been more leaks that we missed.

## Experiment 2

The second time in the lab we let the inlet pressure remain constant and the gap height vary instead of adjusting the inlet pressure to keep the gap height constant. We also used much lower applied masses on our bearings so that any unidentified leaks would not be magnified.

The first run was for the flat bearing. The mass of this bearing was found to be 0.15985 kg. We subjected the bearing to the applied loadings of 0.00, 0.020, 0.040, 0.060, 0.080, 0.100, 0.120, 0.140, 0.160 and 0.180 kg. When the pressure versus mass for this bearing was graphed, as in Appendix D, Figure 4, a linear relationship between those two quantities was clearly observed. This means that we can compare the slope of this graph to the slope of pressure versus mass plots for other bearings to see which bearing is more efficient. The slope for this particular plot for the flat bearing was 9417.1 Pa/kg. All of the slopes derived from the experimental data were achieved using a least squares fit in Microsoft Excel.

Our next run was with the annular bearing of mass 0.15981 kg. The thickness of the shim stock used to create the annulus was 0.00254 cm. We subjected it to the applied loadings of 0.00, 0.020, 0.060, 0.100, 0.140 and 0.180 kg. As expected, this bearing also exhibited a linear relationship between pressure and mass. The plot for this can be seen in Appendix D, Figure 5.

Here we have shown experimentally that the pressure does indeed have a linear relationship with the mass. This means that we can predict the slope for bearings with different bottom surface designs. Theoretically, for a given value of  $\epsilon$ , equations 6.3 and 7.6 can be used to predict the slope for flat bearings of given diameters and annular bearings of known geometries respectively. Using the slope for the 10.16 cm flat bearing (9417 Pa/kg) and equation 6.3, the experimental value for the effective inlet diameter,  $\epsilon$ , was calculated to be 0.11 cm. However, if one would like to predict the slope for a bearing of a given geometry and then verify the result experimentally,  $\epsilon$  needs to be calibrated for that particular laboratory run. This is necessary because  $\epsilon$  varies with the flow rate which varies between experiments, as we have no way of accurately measuring the flow rate with the equipment available to us.

When we compare the slope of pressure versus mass for this bearing, which is 8004.1 Pa/kg, to that of the flat bearing, 9417.1 Pa/kg, we see that the slope for this bearing is the shallower of the two (see Figure 6). This result was expected because the annulus should theoretically trap more of the higher pressured air underneath the bearing, providing better lift. Since the slope is shallower for the annular bearing, more weight can be applied per unit of applied pressure than for the flat bearing case.

### Experiment 3

This time in the lab we used three different bearings, a 10.16 cm diameter flat bearing, a 10.16 cm diameter bearing with an annulus of 2.54 cm radius and a 15.24 cm diameter flat bearing. We kept the flow rate the same for all the bearings so that we could determine  $\epsilon$  from the 10.16 cm flat bearing and use that value to calculate the slope of the two other bearings using equation 6.3 for the 15.24 cm flat bearing and equation 7.6 for the 10.16 cm annular bearing.

The value for  $\epsilon$  that was determined from the 10.16 cm flat bearing is 0.299 cm. Using this to calculate the slope for the 15.24 cm diameter flat bearing we get 3484.6 Pa/kg, which is very close to the value that is obtained through the plotting the experimental data, 3307.9 Pa/kg. When we use that  $\epsilon$  to approximate the slope for the 10.16 cm diameter bearing with annular radius of 2.54 cm we get 4489 Pa/kg, which is very close to the experimental value of 4977 Pa/kg.

This experiment proves to us that we can calculate  $\epsilon$  from the 10.16 cm flat bearing and use it to calculate the slope for other flat bearings and for bearings with one annulus in order to determine if one design is better than another. We could not get this to work correctly at first for the annular case due to the fact that the lift equation we were using was incorrect. After re-deriving that equation, it now gives much better approximations. The graphs of pressure vs. mass for these three bearings can be seen Figures 8, 9 and 10 in Appendix E.

#### Experiment 4

The last experiment we ran was with the 10.16 cm flat bearing and four annular bearings. Three of the four annular bearings have an  $h_1$  value of 0.00254 cm and  $r_1$  values of 1.905, 2.54 and 3.175 cm. The other annular bearing has an  $h_1$  value of 0.00762 cm and an  $r_1$  value of 2.54 cm. Just as before, we kept the flow rate constant for all of these bearings, but this was not necessary because we cannot accurately measure  $h_2$  in the lab.

For the three bearings with the  $h_1$  value of 0.00254 cm, we expected the pressure versus mass slope to decrease as the radius of the annulus increased. This did not exactly happen however. The slope for the bearing with  $r_1 = 1.905$  cm was found to be 4678.1 Pa/kg, while the slope for the bearing with  $r_1 = 2.54$  cm is 4959.3 Pa/kg and the slope for the bearing with  $r_1 = 3.175$  cm is 4819.6 Pa/kg. This says that the bearing with the smallest radius annulus of the three is the best design, but this is not what we anticipated to happen. Our intuitive belief that the bearing should have a better design with the same  $r_1$  value and a greater  $h_2$  value was confirmed, though. The bearing with  $r_1 = 2.54$  cm and  $h_2 = 0.00254$  cm had a slope of 4959.3 Pa/kg, while the bearing with the same  $r_1$  value but  $h_2$  value of 0.00762 cm had a slope of 4136.2 Pa/kg. The graphs of pressure vs. mass for all of these bearings can be seen Figures 11 through 15 in Appendix F.

#### ***Lab Conclusion***

After completing all of these experiments, we feel that we are headed in the right direction. We could not test the optimum single annular case in the lab because we were not able to solve for it. Everything that we have done so far in the lab has helped push us

towards finding a solution for that case, but due to time constraints we did not get to that point.

## Conclusions

An error was found in the previous work conducted toward annular optimization. The analytical solution for the lift was derived using incorrect constraints. After re-deriving the equation, the solution was found to be Equation 7.7. Using this equation, the experimental slope for the original annular case where  $R_1 = 2.54$  cm was predicted within a reasonable range (4489 theory; 4977 experimental), contrary to previous findings. The previous solution predicted values close to 2000.

However, using this new equation, we are still not able to make direct connections between the lift predicted by the computer program and the lift predicted by the analytical solution. Additionally, when the volume constraint is applied to the non-dimensional solution, a plot of the pressure vs. H has a singularity around  $H=0.3$  and negative values for pressure after this point as shown in Figures G and H below.

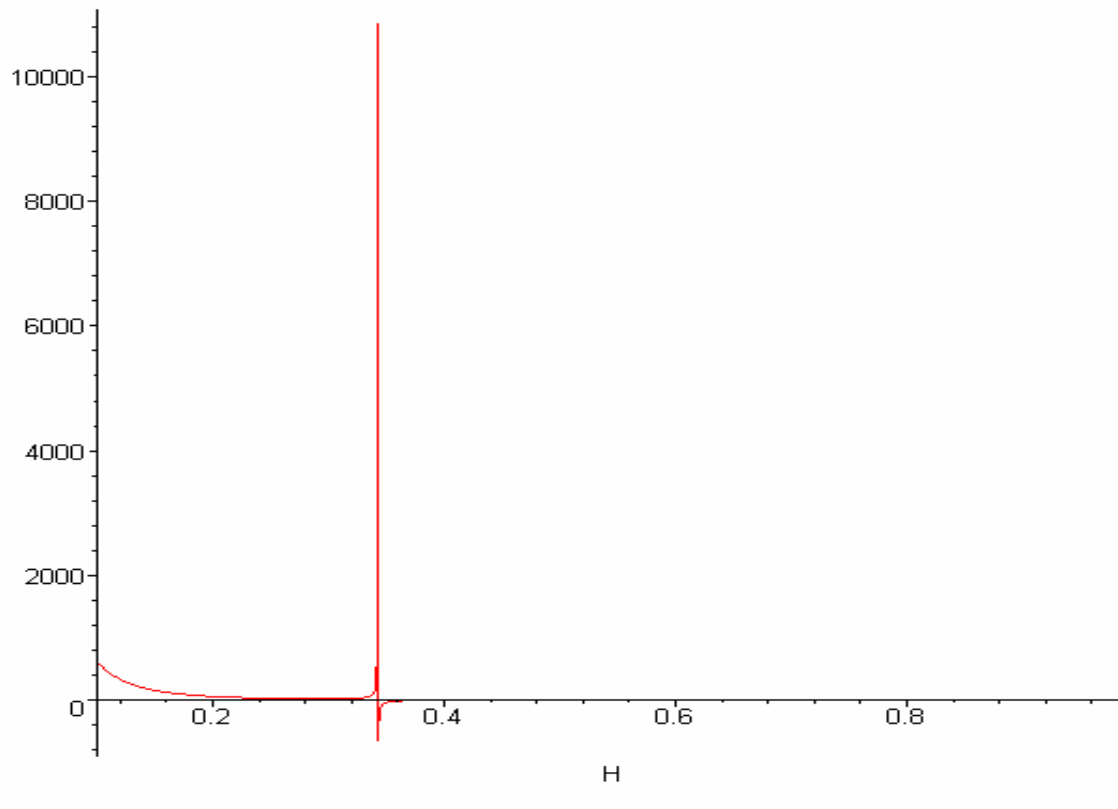


*Figure G.* Maple plot of pressure vs. the ratio  $H$ . The singularity and the lack of pressure values after this point seem indicative of another problem with the derived solutions. See Appendix H for the complete Maple worksheet.

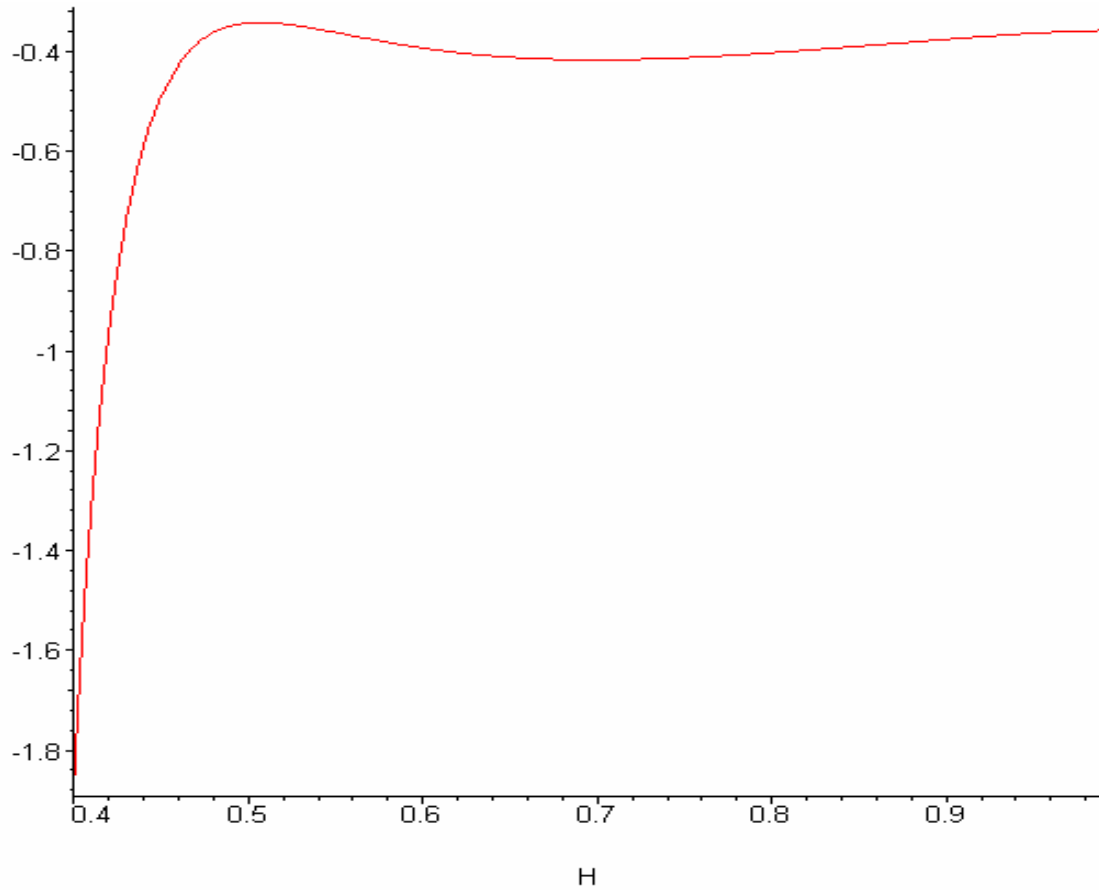


*Figure H.* Maple plot of pressure for  $H=0.4$  to  $0.99$ . Note the negative values indicated for pressure.

To move forward with this problem, the validity of the assumptions made should be reconsidered. Additionally, the volume constraint should be critically analyzed.

## Appendix A

### Annotated Bibliography

- 1) Cameron. *Basic Lubrication Theory, 2<sup>nd</sup> Edition*. Ellis Horwood Limited, England, 1976.

This book outlines basic mechanisms of lubrication. Reynolds equation is derived and discussed in detail, which is of particular value for our purposes. Oil is the primary mode of lubrication discussed in the book in conjunction with several different types of bearings. Pressure equations are discussed for most of the bearings that the book focuses on. These equations may be good references as we develop our model further.

- 2) Szeri, Andras Z. *Fluid Film Lubrication Theory & Design*. Cambridge University Press, New York, 1998.

This book primarily discusses various bearings and methods of lubrication. The text does a good job of discussing the material from a fluid mechanics standpoint. The Reynolds Equation is discussed, along with Navier-Stokes Equations and the Equation of Continuity. Points of interest in the text include some optimization discussion and flow stability. The book also covers non-Newtonian fluids as well as gas lubrication, either of which topics may be useful as model development and refinement continues.

- 3) Grassam, N.S., Ed. and Powell, J.W., Ed. *Gas Lubricated Bearings*. Butterworths, London, 1964.

Points of interest included in this reference are the design of aerodynamic bearings, the design of externally pressurized bearings, and dynamic characteristics of externally pressurized bearings. This book will be of more use to the team as we refine the problem. The compressibility of gas is taken into account for most of the applications of this book. At the beginning stages of the model development we are assuming gas to be

incompressible. If we choose to alter this assumption at some point, this reference may be of use.

- 4) Pinkus, Oscar and Sternlicht, Beno. *Theory of Hydrodynamic Lubrication*. McGraw-Hill Book Company, Inc., 1961.

Highlights in this book include basic differential equations, motion for compressible and incompressible fluids, gas bearings, hydrodynamic instability, non-Newtonian fluids, and experimental evidence. This reference is heavy on mathematical theory and derivation, which will be of use for the model development. Techniques for numerical analysis of Reynolds equation are outlined which will prove very useful for the project.

- 5) Chan, W.K. and Sun, Yuhong. "Analytical Modeling of Ultra-thin-film Bearings." *Journal of Micromechanics and Microengineering* 2003;13;463-473.

This journal article proposes an improved analytical model for ultra-thin-film bearings based on the kinetic theory of gases. The model used in this document, however, takes slip into account, whereas we are assuming no slip in our model. The useful information from this article is the modified Reynolds equations that are used and the fact that they look at flow rate versus the inverse Knudsen number for a wide range of Knudsen numbers. The Knudsen number is defined as the ratio of the mean free path to the characteristic height. The flow rate at such a small gas thin-film thickness has a very different behavior than that of macroscopic gas flow. This digression is measured by the Knudsen number. We will have to take this into account as our research and model development continues.

- 6) Galdi, Giovanni, Ed., Heywood, John, Ed., and Rannacher, Rolf, Ed. *Fundamental Directions in Mathematical Fluid Mechanics*. Birkhauser Verlag, Basel, 2000.

This book includes sections on Navier-Stokes initial-boundary value problems, spectral approximations of Navier-Stokes equations, and finite element methods for the incompressible Navier-Stokes equations. As the Navier-Stokes equations are the equations of motion for an

incompressible, Newtonian fluid, the solver techniques this text provides have great potential for use in this project. In particular, the section on spectral methods may come of use when trying to solve for the finite pressure distribution over a circular region as the optimization deals with.

- 7) Griebel, Micheal, Dornseifer, Thomas, and Neuhoefter, Tilman. *Numerical Simulation in Fluid Dynamics: A Practical Introduction*. SIAM, Philadelphia, 1998.

Useful aspects of this book are mathematical descriptions of flows, numerical treatment of Navier-Stokes equations, and some example applications. Again, at this phase in the project, there is some emphasis on learning numerical techniques that can be applied to fluid mechanics and dynamics.

- 8) Edwards, Dilwyn and Hamson, Mike. *Guide to Mathematical Modeling*. CRC Press, Inc., Boca Raton, 1990.

This resource is not directly related to the problem at hand but rather helps with the methodology of solving problems in general. The book discusses the use of differential equations in modeling and provides some helpful examples.

- 9) Bulirsch, R., Ed., Miele, A., Ed., Stoer, J., Ed., and Well, K.H., Ed. *Optimal Control: Calculus of Variations, Optimal Control Theory and Numerical Methods*. Birhauser Verlag, Basel, 1993.

This book will become useful as optimization is further sought. Topics include, optimality conditions and algorithms, numerical methods, and analysis and synthesis of nonlinear systems. Also, there is a section reserved for applications to mechanical and aerospace systems. The examples within this section are optimizations for real-life applications which will be useful in trying to optimize the real-life problem of the air bearing.

10) Trefethen, Lloyd N. *Spectral Methods in MATLAB*. Society for Industrial and Applied Mathematics, 2000.

This book is useful as we work towards using numerical methods to solve the governing equations of our problem. It focuses on spectral methods which can be applied to irregular geometries such as the circular geometry relevant in the air bearing problem. The book is also full of MATLAB code which we can build on and modify for our applications.

## Appendix B

**with (VectorCalculus) ;**

Warning, the assigned names <, > and <|> now have a global binding

Warning, these protected names have been redefined and unprotected: \*, +, ., Vector, diff, int, limit, series

[&x, \*, +, ., <,>, <|>, AddCoordinates, ArcLength, BasisFormat, Binormal, CrossProduct, Curl, Curvature, Del, DirectionalDiff, Divergence, DotProduct, Flux, GetCoordinateParameters, GetCoordinates, Gradient, Hessian, Jacobian, Laplacian, LineInt, MapToBasis, Nabla, PathInt, PrincipalNormal, RadiusOfCurvature, ScalarPotential, SetCoordinateParameters, SetCoordinates, SurfaceInt, TNBFrame, Tangent, TangentLine, TangentPlane, TangentVector, Torsion, Vector, VectorField, VectorPotential, Wronskian, diff, evalVF, int, limit, series]

**SetCoordinates ('polar' [r, theta]) ;**  
*polar*<sub>r, θ</sub>

**P:=Gradient (p (r, theta) , 'polar' [r, theta]) ;**

$$P := \left( \frac{\partial}{\partial r} p(r, \theta) \right) \bar{\mathbf{e}}_r + \frac{\frac{\partial}{\partial \theta} p(r, \theta)}{r} \bar{\mathbf{e}}_\theta$$

**F := (h (r, theta) ) ^3 \* P ;**

$$F := h(r, \theta)^3 \left( \frac{\partial}{\partial r} p(r, \theta) \right) \bar{\mathbf{e}}_r + \frac{h(r, \theta)^3 \left( \frac{\partial}{\partial \theta} p(r, \theta) \right)}{r} \bar{\mathbf{e}}_\theta$$

**Divergence (F) ;**

$$\left( h(r, \theta)^3 \left( \frac{\partial}{\partial r} p(r, \theta) \right) + 3 r h(r, \theta)^2 \left( \frac{\partial}{\partial r} p(r, \theta) \right) \left( \frac{\partial}{\partial r} h(r, \theta) \right) + r h(r, \theta)^3 \left( \frac{\partial^2}{\partial r^2} p(r, \theta) \right) + \frac{3 h(r, \theta)^2 \left( \frac{\partial}{\partial \theta} p(r, \theta) \right) \left( \frac{\partial}{\partial \theta} h(r, \theta) \right)}{r} + \frac{h(r, \theta)^3 \left( \frac{\partial^2}{\partial \theta^2} p(r, \theta) \right)}{r} \right) / r$$

**simplify(%) ;**

$$h(r, \theta)^2 \left( h(r, \theta) \left( \frac{\partial}{\partial r} p(r, \theta) \right) r + 3 r^2 \left( \frac{\partial}{\partial r} p(r, \theta) \right) \left( \frac{\partial}{\partial r} h(r, \theta) \right) + r^2 h(r, \theta) \left( \frac{\partial^2}{\partial r^2} p(r, \theta) \right) + 3 \left( \frac{\partial}{\partial \theta} p(r, \theta) \right) \left( \frac{\partial}{\partial \theta} h(r, \theta) \right) + h(r, \theta) \left( \frac{\partial^2}{\partial \theta^2} p(r, \theta) \right) \right) / r^2$$

## Appendix C

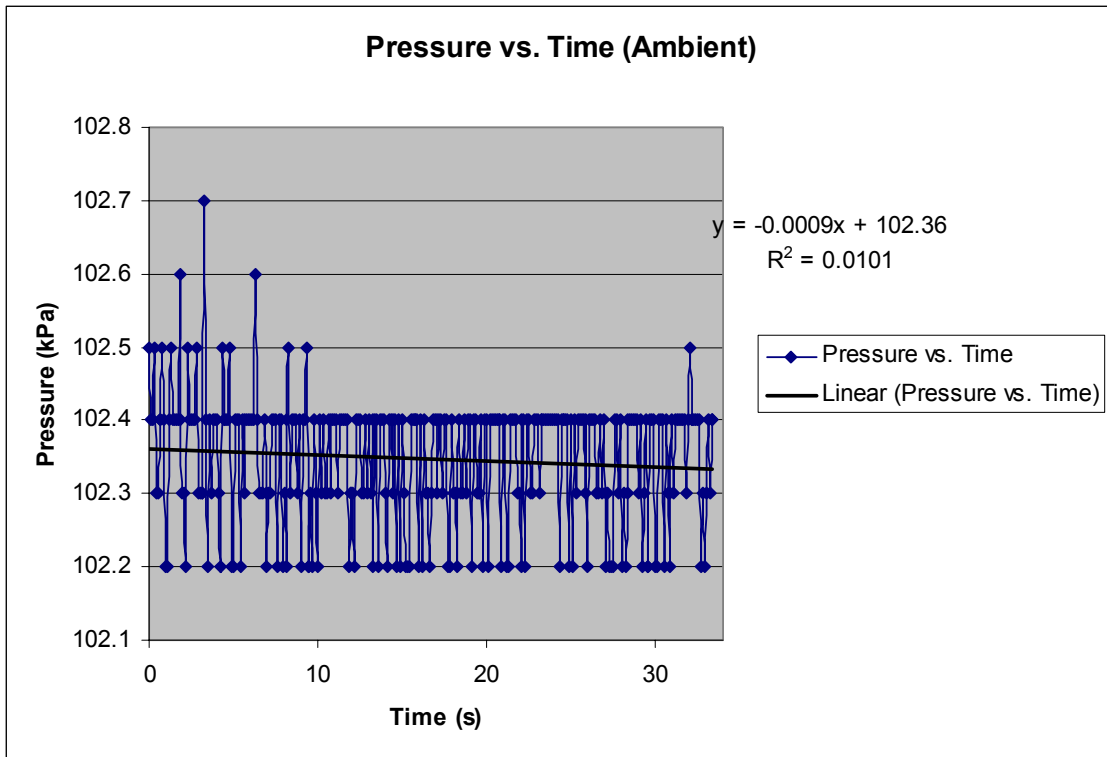
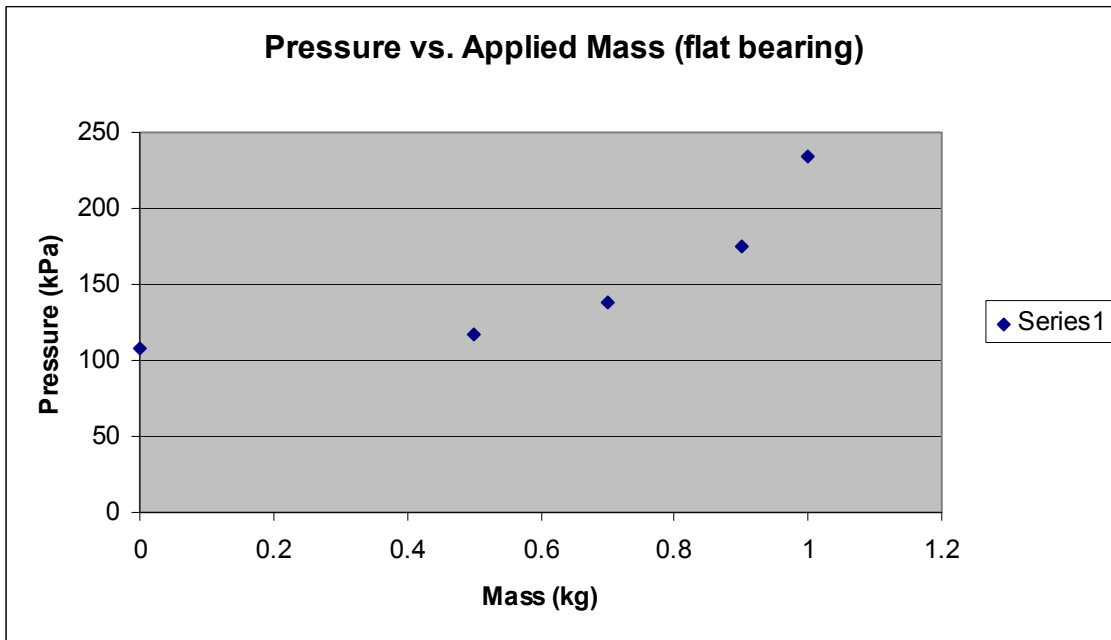
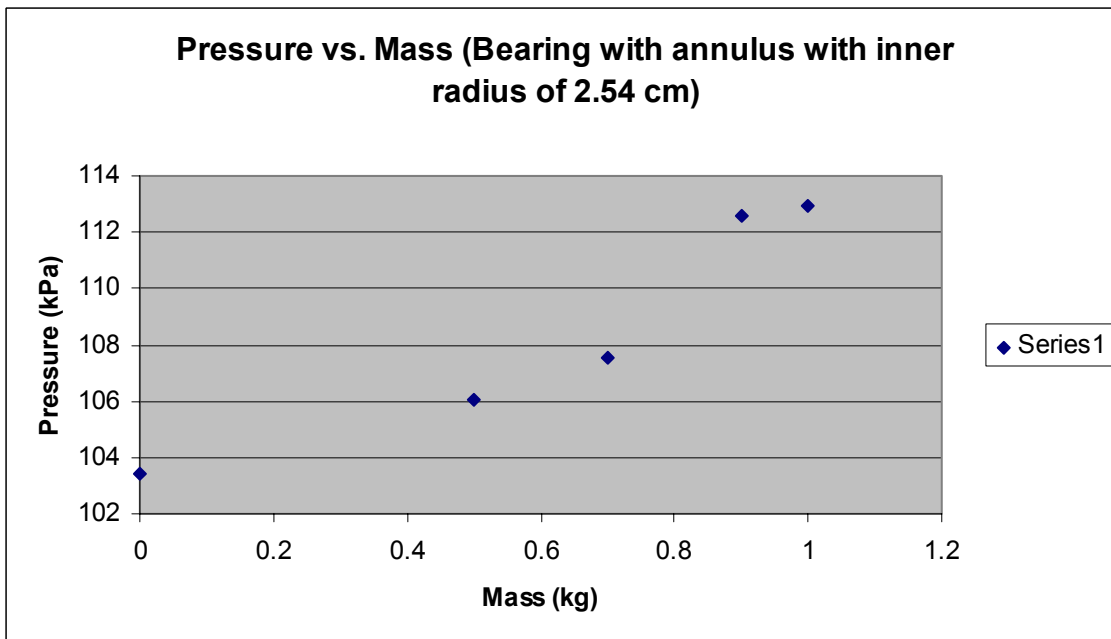


Figure 1



**Figure 2**



**Figure 3**

## Appendix D

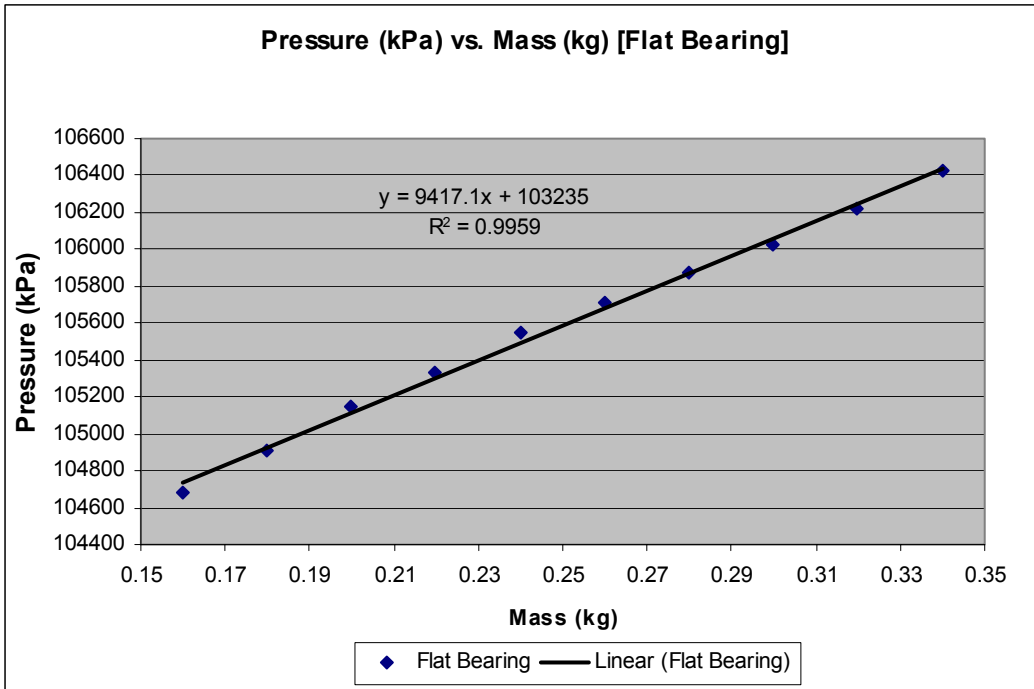


Figure 4

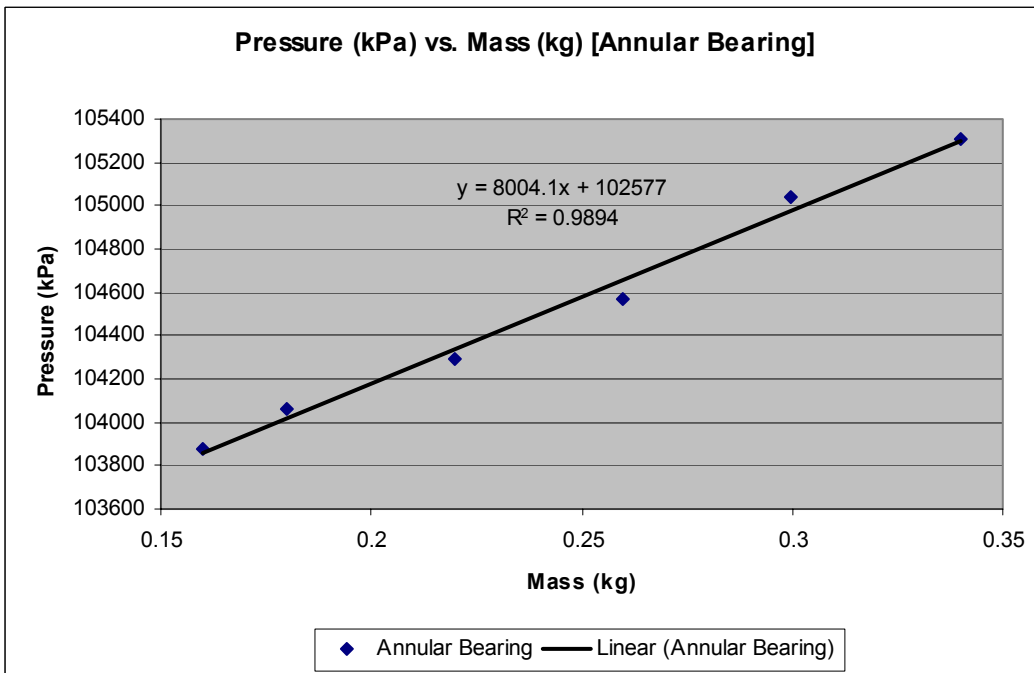


Figure 5

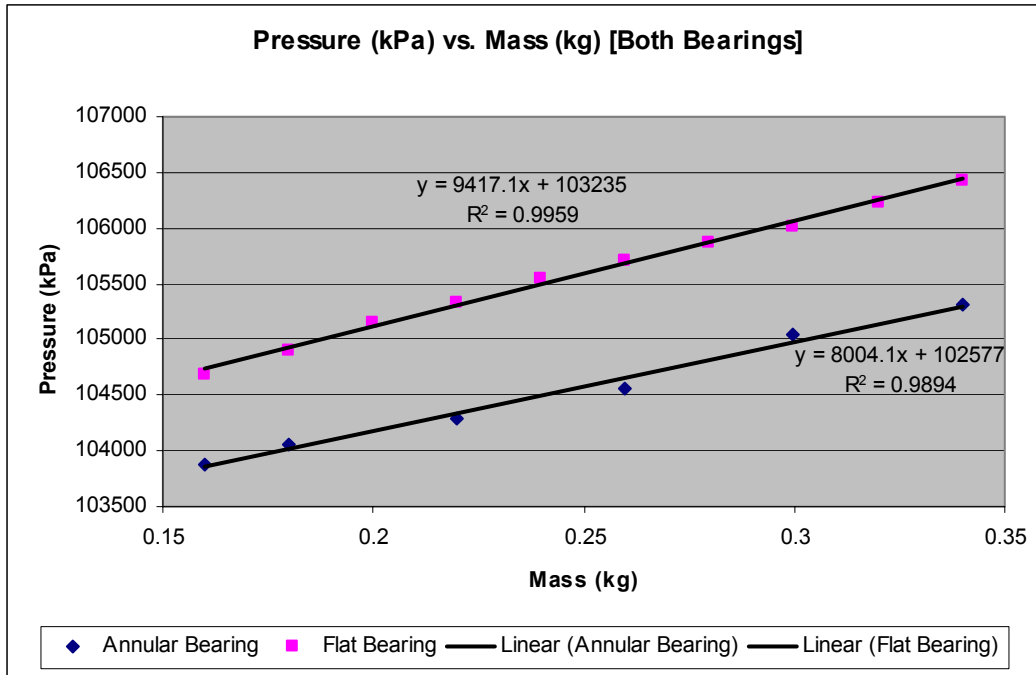


Figure 6

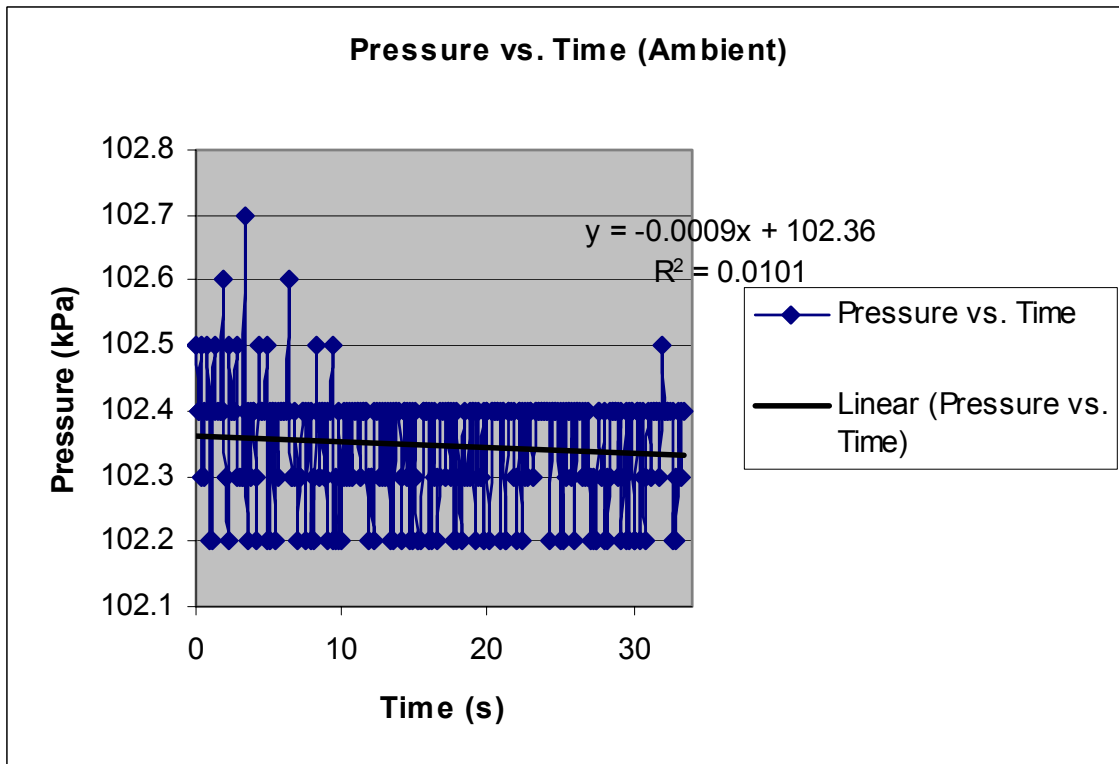


Figure 7

## Appendix E

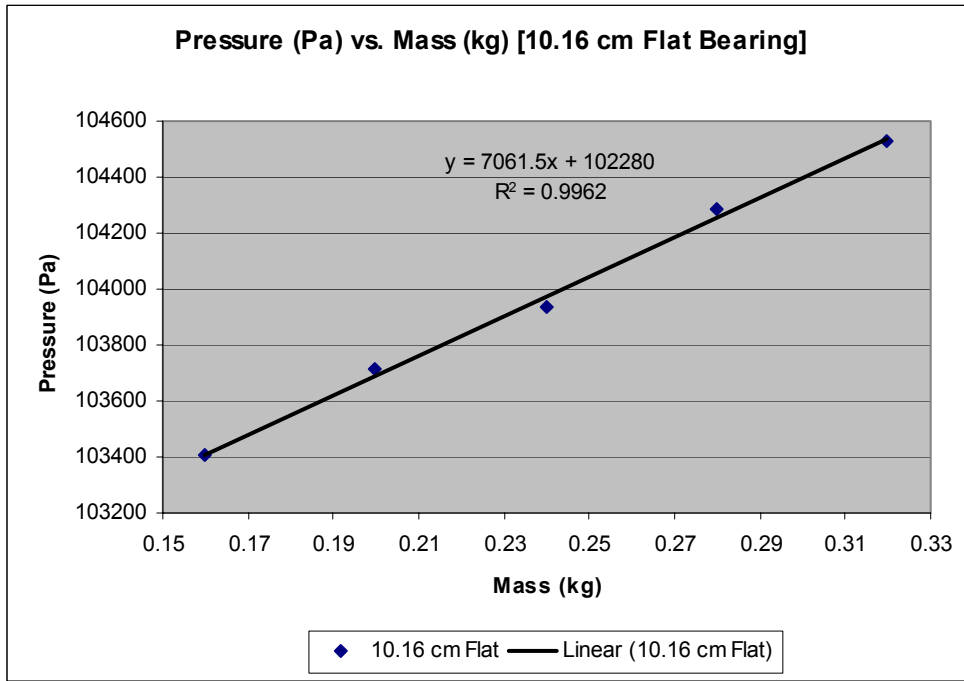


Figure 8

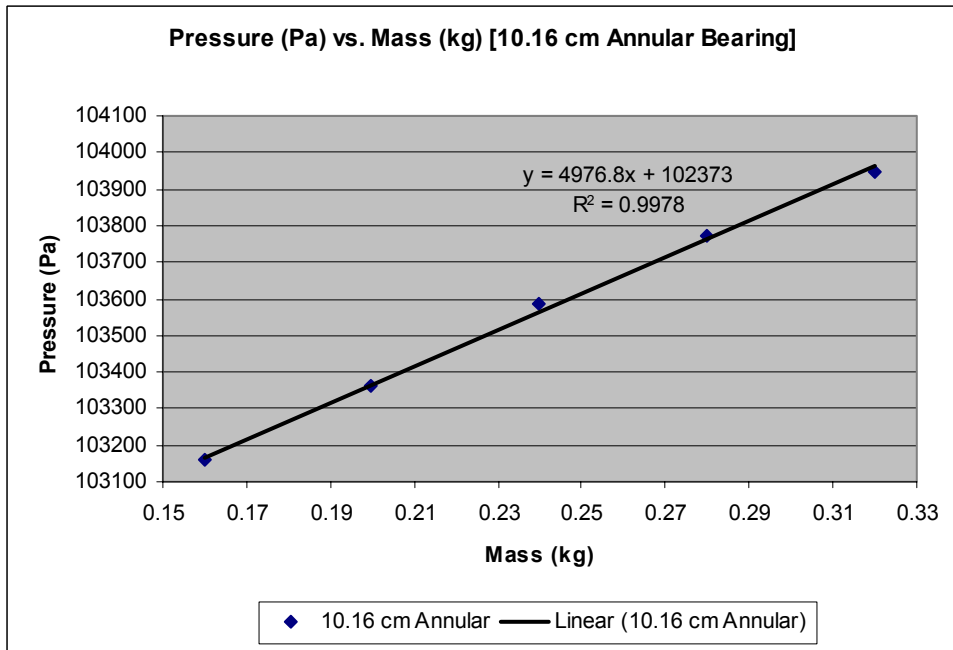
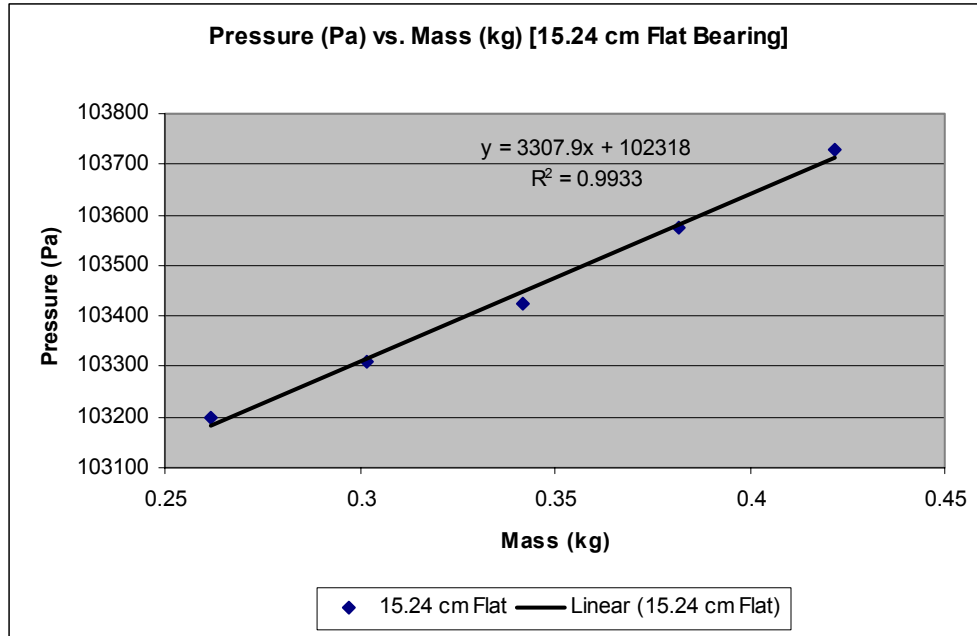


Figure 9



**Figure 10**

## Appendix F

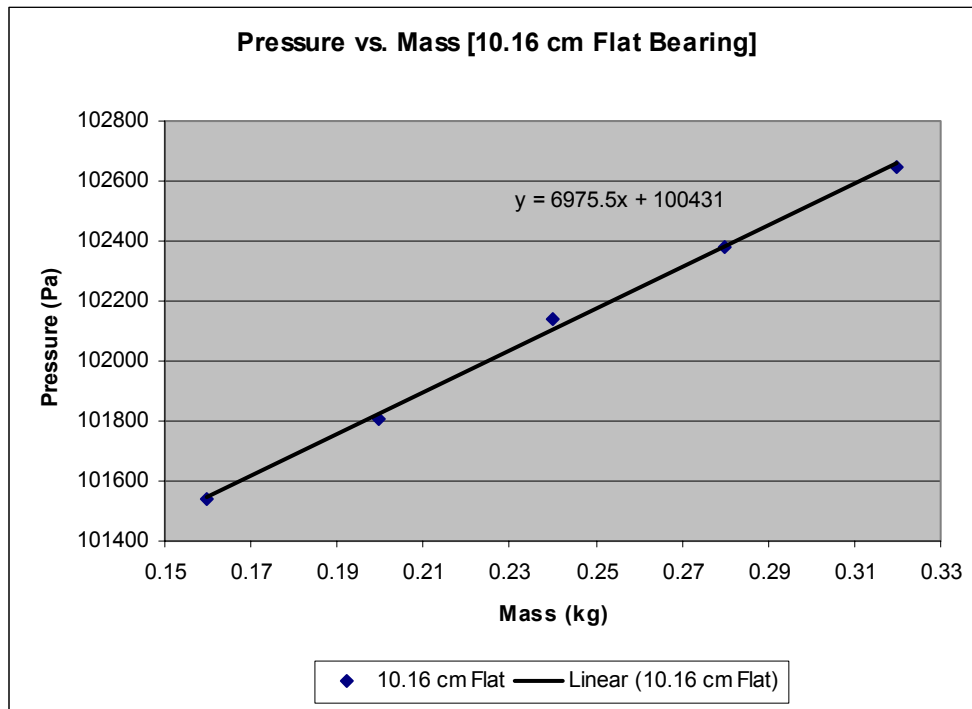


Figure 11

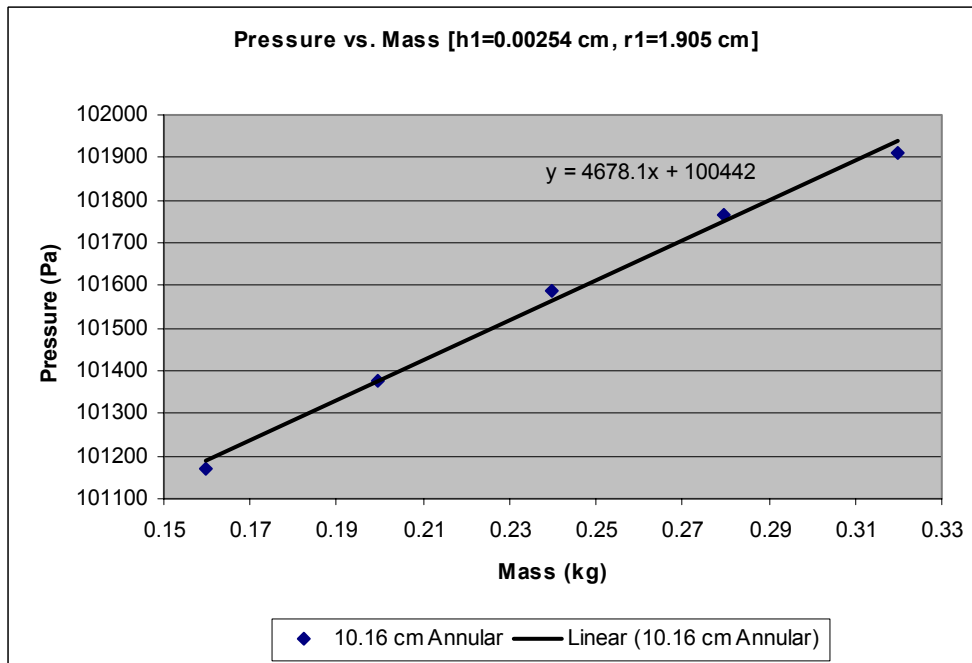
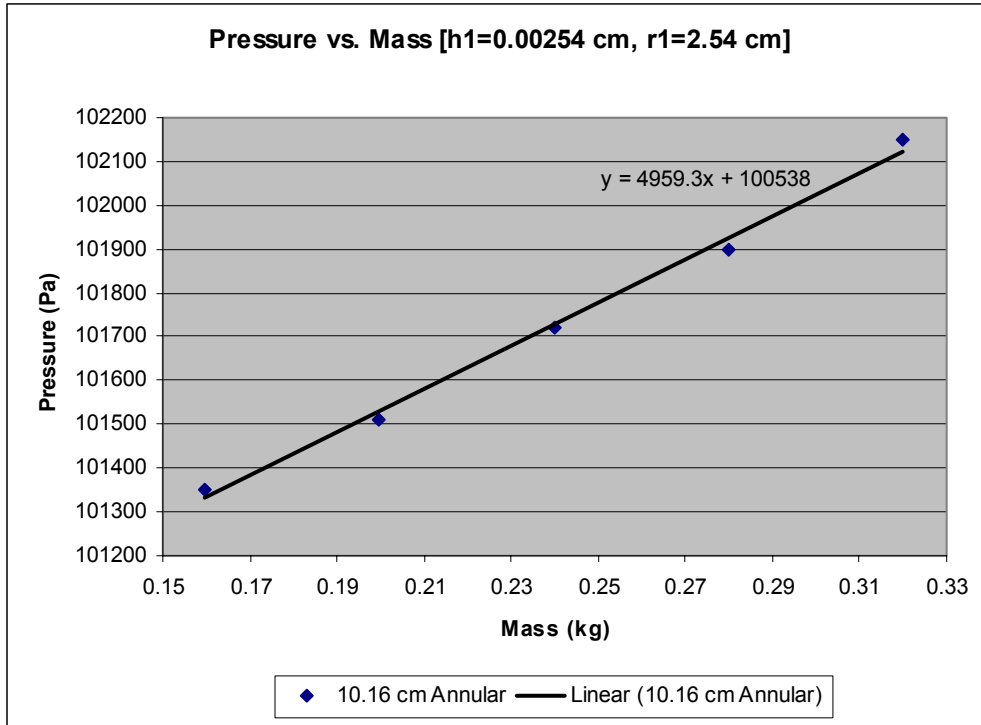
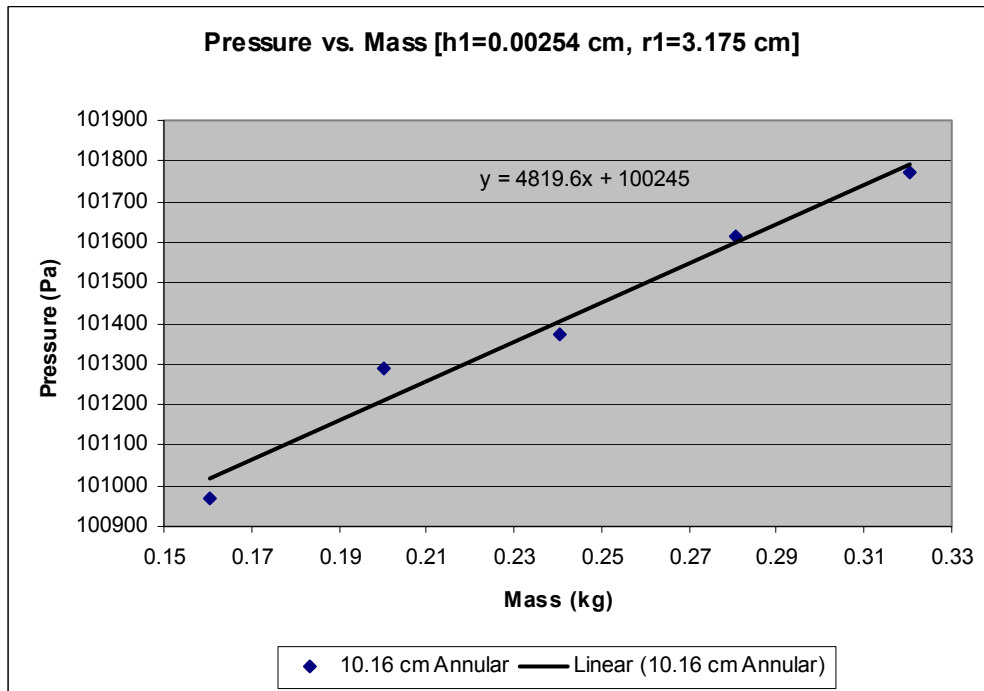


Figure 12



**Figure 13**



**Figure 14**

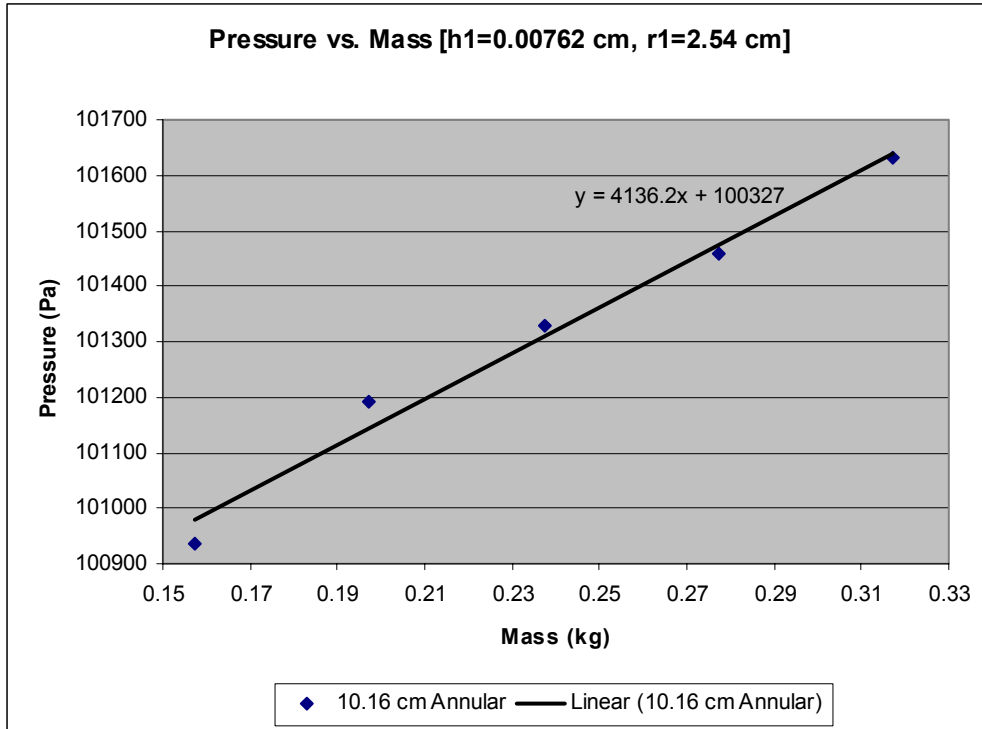


**Figure 15**

## Appendix G

> restart;

> A:=H^3\*P/(ln((R1^((H^(-3))-1)\*epsilon)/R2^(H^(-3))));

$$A := \frac{H^3 P}{\ln \left( \frac{R1 \left( \frac{1}{H^3} - 1 \right) \epsilon}{R2 \left( \frac{1}{H^3} \right)} \right)}$$

>

> I1:=int(int(r\*ln(r/epsilon),r=epsilon..R1),theta=0..2\*Pi);

$$I1 := R1^2 \ln \left( \frac{R1}{\epsilon} \right) \pi - \frac{R1^2 \pi}{2} + \frac{\epsilon^2 \pi}{2}$$

> I2:=int(int(P\*r,r=epsilon..R1),theta=0..2\*Pi);

$$I2 := P (R1^2 - \epsilon^2) \pi$$

> L1:=(A\*I1)+I2;

$$L1 := \frac{H^3 P \left( R1^2 \ln \left( \frac{R1}{\epsilon} \right) \pi - \frac{R1^2 \pi}{2} + \frac{\epsilon^2 \pi}{2} \right)}{\ln \left( \frac{R1 \left( \frac{1}{H^3} - 1 \right) \epsilon}{R2 \left( \frac{1}{H^3} \right)} \right)} + P (R1^2 - \epsilon^2) \pi$$

> C:=P/(ln((R1^((H^(-3))-1)\*epsilon)/R2^(H^(-3))));

$$C := \frac{P}{\ln \left( \frac{R1 \left( \frac{1}{H^3} - 1 \right) \epsilon}{R2 \left( \frac{1}{H^3} \right)} \right)}$$

> I3:=int(int(r\*ln(r/R2),r=R1..R2),theta=0..2\*Pi);

$$I3 := -\frac{R2^2 \pi}{2} - R1^2 \ln \left( \frac{R1}{R2} \right) \pi + \frac{R1^2 \pi}{2}$$

> L2:=C\*I3;

$$L2 := \frac{P \left( -\frac{R2^2 \pi}{2} - R1^2 \ln\left(\frac{R1}{R2}\right) \pi + \frac{R1^2 \pi}{2} \right)}{\ln \left( \frac{R1 \left( \frac{1}{H^3} - 1 \right) \epsilon}{R2 \left( \frac{1}{H^3} \right)} \right)}$$

> L3:=int(int(P\*r,r=0..epsilon),theta=0..2\*Pi);  
L3 := P ε<sup>2</sup> π

> L:=L1+L2+L3;

$$L := \frac{H^3 P \left( R1^2 \ln\left(\frac{R1}{\epsilon}\right) \pi - \frac{R1^2 \pi}{2} + \frac{\epsilon^2 \pi}{2} \right)}{\ln \left( \frac{R1 \left( \frac{1}{H^3} - 1 \right) \epsilon}{R2 \left( \frac{1}{H^3} \right)} \right)} + P (R1^2 - \epsilon^2) \pi$$

$$+ \frac{P \left( -\frac{R2^2 \pi}{2} - R1^2 \ln\left(\frac{R1}{R2}\right) \pi + \frac{R1^2 \pi}{2} \right)}{\ln \left( \frac{R1 \left( \frac{1}{H^3} - 1 \right) \epsilon}{R2 \left( \frac{1}{H^3} \right)} \right)} + P \epsilon^2 \pi$$

> L := H^3\*P/H\*(R1^2\*ln(R1/epsilon)\*Pi-  
1/2\*R1^2\*Pi+1/2\*epsilon^2\*Pi)+P\*(R1^2-  
epsilon^2)\*Pi+P/ln(R1^(1/(H^3))-  
1)\*epsilon/(R2^(1/(H^3)))\*(-1/2\*R2^2\*Pi-  
R1^2\*ln(R1/R2)\*Pi+1/2\*R1^2\*Pi)+P\*epsilon^2\*Pi;  
> l:=M\*g=L;

$$l := M g = \frac{H^3 P \left( R I^2 \ln\left(\frac{R I}{\epsilon}\right) \pi - \frac{R I^2 \pi}{2} + \frac{\epsilon^2 \pi}{2} \right)}{\ln\left(\frac{R I^{\left(\frac{1}{H^3}-1\right)}}{\epsilon}}{\frac{R 2^{\left(\frac{1}{H^3}\right)}}}\right)} + P (R I^2 - \epsilon^2) \pi$$

$$+ \frac{P \left( -\frac{R 2^2 \pi}{2} - R I^2 \ln\left(\frac{R I}{R 2}\right) \pi + \frac{R I^2 \pi}{2} \right)}{\ln\left(\frac{R I^{\left(\frac{1}{H^3}-1\right)}}{\epsilon}}{\frac{R 2^{\left(\frac{1}{H^3}\right)}}}\right)} + P \epsilon^2 \pi$$

> **l1:=solve(l,P);**

$$l1 := 2 M g (\ln(\epsilon) H^3 + \ln(R I) - \ln(R I) H^3 - \ln(R 2)) / \left( \pi \left( 2 H^6 R I^2 \ln\left(\frac{R I}{\epsilon}\right) - H^6 R I^2 + H^6 \epsilon^2 + 2 R I^2 \ln(\epsilon) H^3 + 2 R I^2 \ln(R I) - 2 R I^2 \ln(R I) H^3 - 2 R I^2 \ln(R 2) - R 2^2 H^3 - 2 R I^2 \ln\left(\frac{R I}{R 2}\right) H^3 + H^3 R I^2 \right) \right)$$

>

> **restart;**

> **L:=H^3\*P/ln(R1^(1/(H^3))-1)\*epsilon/(R2^(1/(H^3))))\*(R1^2\*ln(R1/epsilon)\*Pi-1/2\*R1^2\*Pi+1/2\*epsilon^2\*Pi)+P\*(R1^2-epsilon^2)\*Pi+P/ln(R1^(1/(H^3))-1)\*epsilon/(R2^(1/(H^3))))\*(-1/2\*R2^2\*Pi-R1^2\*ln(R1/R2)\*Pi+1/2\*R1^2\*Pi)+P\*epsilon^2\*Pi;**

>

$$L := 0.0006949315102 P \pi$$

> **l:=M\*g=L;**

$$l := 9.81 M = 0.0006949315102 P \pi$$

> **solve(l,P);**

$$4493.421204 M$$

> **R1:=0.0254;**

$$R I := 0.0254$$

> **R2:=0.0508;**

$$R 2 := 0.0508$$

```
> epsilon:=0.00287;
```

```
 $\varepsilon := 0.00287$ 
```

```
> H:=0.5;
```

```
 $H := 0.5$ 
```

```
> g:=9.81;
```

```
 $g := 9.81$ 
```

## Appendix H

> restart;

> P:=(2/Pi)\*((ln(r1^((H^(-3))-1)\*epsilon))/(r1^2\*(1-H^3)+H^3\*epsilon^2-1));

$$P := \frac{2 \ln \left( r l^{\left( \frac{1}{H^3} - 1 \right)} \epsilon \right)}{\pi \left( r l^2 \left( 1 - H^3 \right) + H^3 \epsilon^2 - 1 \right)}$$

> p1:=subs(r1=sqrt(q/(H^(-1)-1)),P);

$$p1 := \frac{2 \ln \left( \left( \sqrt{\frac{q}{\frac{1}{H} - 1}} \right)^{\left( \frac{1}{H^3} - 1 \right)} \epsilon \right)}{\pi \left( \frac{q \left( 1 - H^3 \right)}{\frac{1}{H} - 1} + H^3 \epsilon^2 - 1 \right)}$$

> p2:=subs(q=2,p1);

$$p2 := \frac{2 \ln \left( \left( \sqrt{2} \sqrt{\frac{1}{\frac{1}{H} - 1}} \right)^{\left( \frac{1}{H^3} - 1 \right)} \epsilon \right)}{\pi \left( \frac{2 \left( 1 - H^3 \right)}{\frac{1}{H} - 1} + H^3 \epsilon^2 - 1 \right)}$$

> p3:=subs(epsilon=0.059,p2);

$$p3 := \frac{2 \ln \left( 0.059 \left( \sqrt{2} \sqrt{\frac{1}{\frac{1}{H} - 1}} \right)^{\left( \frac{1}{H^3} - 1 \right)} \right)}{\pi \left( \frac{2 \left( 1 - H^3 \right)}{\frac{1}{H} - 1} + 0.003481 H^3 - 1 \right)}$$

> plot(p3,H=0.1..0.99);

